January 16, 2006

In-flight calibration of the ACIS spectral response

A. Vikhlinin

Abstract

This document describes a new approach to calibration of the spatially-dependent spectral response of the ACIS CCDs.

1 Introduction

The spectral resolution of the ACIS CCDs is a strong funtion of location. This was expected for the Back-Illuminated (BI) chips S1 and S3 because of their high intrinsic Charge Transfer Inefficiency (CTI).[1] Unfortunately, even very-nearly-ideal Front-Illuminated (FI) chips were radiationally-damaged during the first weeks of the *Chandra* mission and now experience strong CTI as well. The systematic charge loss for detected X-ray photons can be mitigated using the so-called CTI correction procedure [2, 3, 4]. However, CTI correction cannot fully restore the energy resolution of the FI CCDs to the pre-flight levels and the resolution remains a strong function of position.

Both mathematical model and in-flight calibration data provide sufficient information for accurate calibration of the ACIS response, as discussed below (§2). The main obstacle in the this work proved to be related to the *representation* of the response data in the calibration products which was tailored to the pre-flight ACIS performance and implemented in the CXC software.

In 2001, we developed a new approach for representation of the ACIS response which was design to mimic the physical processes responsible for the spatial variations of the spectral resolution. This approach proved to be very fruitful and resulted in significant calibration improvements, as documented below.

1.1 Previous approaches to representation of ACIS spectral response

1.1.1 Analytic representation (FEF)

Based on the pre-flight calibration, a paradigm referred to as the FITS Embeddeed Functions (FEF) was developed and implemented in the CXC software (MKRMF). Essentially, the spectral redistribution function was represented analytically as a set of 10 Gaussians at several reference energies, E^j, and the parameters of these Gaussians were stored in the FITS table. To calculate the response at an intermediate energy, E, one obtains the parameters for 10 Gaussians at the desired location by interpolation from the reference points and then actually computes the function:

$$\begin{aligned} \mathrm{LOC}_i &= w^j\,\mathrm{LOC}_i^j + w^{j+1}\,\mathrm{LOC}_i^{j+1} \\ \mathrm{WIDTH}_i &= w^j\,\mathrm{WIDTH}_i^j + w^{j+1}\,\mathrm{WIDTH}_i^{j+1} \\ \mathrm{AMPL}_i &= w^j\,\mathrm{AMPL}_i^j + w^{j+1}\,\mathrm{AMPL}_i^{j+1} \end{aligned} \tag{1}$$

and then

$$\mathrm{RESP}\,(\mathrm{CHAN}, E) = \sum_{i=1,10} \mathrm{AMPL}_i \times \exp\left(-\frac{(\mathrm{CHAN}-\mathrm{LOC}_i)^2}{2\,\mathrm{WIDTH}_i^2}\right), \tag{2}$$

where $w^j = (E^{j+1} - E)/(E^{j+1} - E^j)$ and $w^{j+1} = 1 - w^j$. This process is very simple mathematically but is not tailored to the physics of the CCD response:

- For the FEF representation to be successful it is necessary that the components have the same "meaning" at all energies (e.g., component 1 should always represent the main peak, component 2 is responsible for the Si-K fluorescence line etc.). In practice, this was found hard to achieve algorithmically when the data was fit using standard software packages; a significant amount of careful hand-editing was required to produce the final tables of the best-fit parameters.

[1] Hereafter, we refer the reader to the Science Instrument Calibration Report [1]

- The situation is additionally complicated by non-smooth behavior of the CCD response around some energies where individual components appear, disappear or "collide".
- Finer details of the spectral redistribution function cannot be represented by a set of 10 Gaussians. This can be mitigated by introduction of additional functional components but this path is non-general and quickly leads to uncontrollable increase in the complexity of the FEF representation.

Even with these caveats in mind, it should be aknowledged that the FEF represenation seemed adeaquate based on the preflight expectations, mainly because the FI chips were so uniform that only one set of FEFs per CCD node was required and FEFs for different nodes were scaled versions of one another. Most important, it was not generally expected that the FEFs will have to be re-created.

Unfortunately, the new set of FEFs had to be created after the FI CCDs experienced the radiation damage. This process proved to be extremely labor-consuming. Compared with creation of a single FEF, the amount of effort increased by a factor of 32 (because 32 RMFs per node were required to accurately follow the spatial variations of the energy resolution) times additional factor of ~ 20 (because every CCD node was damaged slightly differently) times another factor of a few (to correct bugs because *errare humanum est*). In fact, FEFs appropriate for CTI-corrected ACIS data were never completed.

The analytic represenation of the RMF does have an important advantage — the RMFs can be "tweaked" relatively easily to better match the observed detector performance. For example, the effective energy resolution (FWHM) can be increased simply by scaling widths of the Gaussian components respresenting the main peak.

1.1.2 Ready-to-use simulated RMFs

2 Available data

2.1 In-flight calibration data

2.2 Monte-Carlo model of ACIS response

3 Factorization of the ACIS response

3.1 Motivation

Motivation (from C. Grant & L. Townsley's memo):

> The addition of CTI correction to the tools available to the Chandra user community, while beneficial scientifically, doubles the number of basic ACIS calibration products. The current paradigm of response matrix generation in which the response is parameterized in the FEF file allows for much flexibility in rebinning and interpolating the products but is expensive in terms of the manpower required to produce the calibration. We would like to recommend that the CXC consider an alternate method, that of producing RMFs and ARFs directly from simulated event lists. ...The benefit of this approach is that the same simulated event lists can be used to produce response matrixes for any subset of the events, such as filtering by position or event grade, and for either CTI corrected or uncorrected events.

Problems:

- the brute force simulations require huge investments of the computer power. From Broos & Townsley's notes on their RMF generation: "the 4×10^8 events we generated for the matrix described here consumed ~ 1100 hours of CPU time" (they simulated just 8 matrices per chip and still their RMFs are quite noisy). Potentially, the simulations will have to be redone after each change in `acis_process_events`.
- it is not clear how to tweak the simulated events to reproduce the calibration observations.

These problems motivate an exploration of a technique which, starting from the simulated event lists of a manageable size, would find the analytic representation of the RMFs (similar to the FEFs approach) without a substantial human intervention.

3.2 Outline of the method

The main idea is to separate the position-dependent and position-independent effects in the RMF. Consider the path of an X-ray photon with energy E in the ACIS detector (Fig. 1). The absorption of the photon in the detector results in formation of the

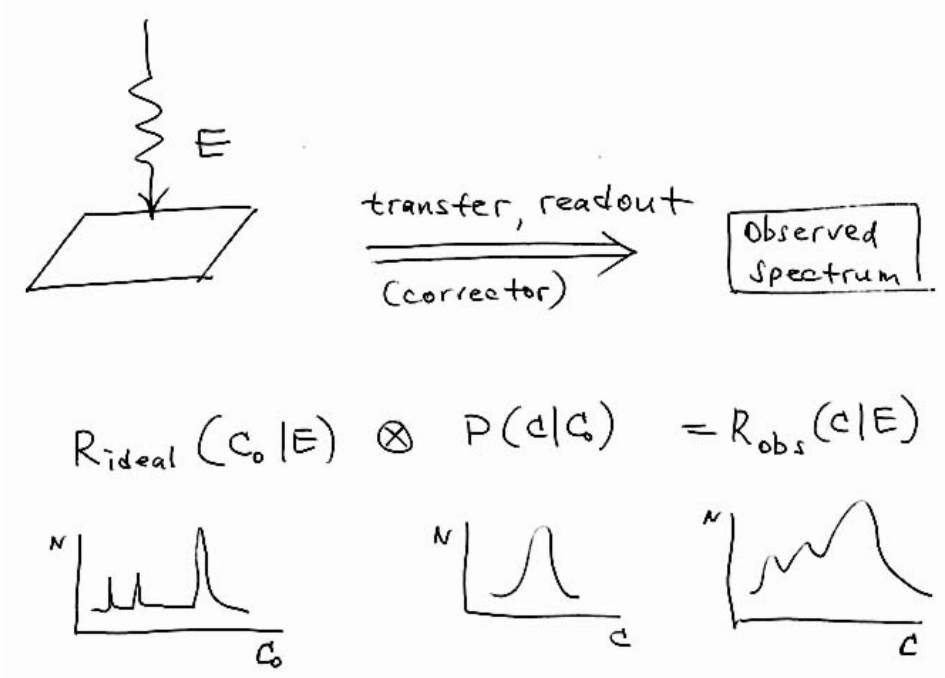

Fig. 1—

electron cloud; the probability density function of the total charge, C_0, can be thought of as an ideal response, $R_{\rm ideal}(C_0|E)$; in the absence of the CTI effects, $R_{\rm ideal}(C_0|E)$ would represent the response matrix. Note that $R_{\rm ideal}(C_0|E)$ is a complex, multi-peak function, which undergoes abrupt changes at certain energies. However, it does not depend on the chip position.

As the chip is read out, the charge cloud is subject to the serial and parallel CTI. It is these processes that result in the degradation of the spectral resolution and its dependence on the chip position. Mathematically, we can represent this by the probability density function $P(C|C_0)$ for the photon to end up in the PHA channel C given the original charge of the cloud C_0 [$P(C|C_0)$ is a function of the chip position]. The observed degraded response $R_{\rm obs}$ is a convolution of $R_{\rm ideal}$ and P:

$$R_{\rm obs}(C,E) = R_{\rm ideal}(C_0|E) \otimes P(C|C_0). \tag{3}$$

The important point is that $P(C|C_0)$, as produced by the ACIS simulator, is a simple, single-peak function with a monotonic dependence on C_0 (the reason for that is a rather simple phenomenological model of the CTI effects built in the simulator). The positional dependence of $R_{\rm obs}$ is entirely due to $P(C|C_0)$, which suggests that instead of calibrating multiple complex matrices $R_{\rm obs}(C,E)$ (hundreds per chip), we can calibrate a single complex matrix $R_{\rm ideal}(C_0|E)$ and multiple simple matrices $P(C|C_0)$. This process can be made fully automatic and computationally efficient.

3.3 The "pha scatter" matrix $P(C|C_0)$

The scatter matrix $P(C|C_0)$ is a unimodal, smooth function of energy. It can be easily represented by an analytic model.

There are two approaches to obtain $P(C|C_0)$.

1) One can use the ACIS simulator with the `add_cti.pro` script to simulate the PHA scatter caused by the CTI. This approach has been used for the 5 FI chips. The simulated scatter matrices are adequately represented as a sum of two gaussians.

2) An analytic model can be devised and fit to the ECS data directly. I use this approach for the BI CCDs (the scatter matrix represented by a single Gaussian) and now for the FI CCDs (scatter matrix represented by a modified King law).

3.4 Computing the degraded response $R_{\rm obs}(C|E)$.

Suppose the ideal response $R_{\rm ideal}(C|E)$ is known. The recipe for computing the degraded RMF $R_{\rm obs}(C|E)$ is:

1. Simulate the distributions of $C - C_0$ for a number of input energies (or, equivalently, C_0's). Fit them with eq. (**??**) and tabulate the best-fit parameters.
2. Interpolate the best-fit functions to obtain the matrix $P(C|C_0)$ in the entire range of C_0.
3. $R_{\rm obs}(C|E)$ is obtained by the matrix multiplication (eq. 3).

3.4.1 Interpolation of analytic fits to $P(C|C_0)$

The best fit parameters in eq. (**??**) change rather smoothly as a function of the input photon energy. Therefore one could interpolate the tabulated parameter values to compute the distribution $P(C|C_0)$ for all C_0's. However a better and more stable approach is to interpolate the functions directly. A possible method for that is the so called contour interpolation. For a pair of functions $f_1(x)$ and $f_2(x)$ one finds the locations, x_i^1 and x_i^2, of the given set of intensity levels, f_i, relative to the maximum. The linear interpolation of $f^1(x)$ and $f^2(x)$ with weights w_1 and w_2 is performed by finding the locations of the intensity levels $x_i = w_1 x_i^1 + w_2 x_i^2$ and the linear interpolation of intensities between them. An example is shown in Figure **??**, where the black curve is the interpolation of the two red curves with equal weights.

With the contour interpolation approach, eq. (**??**) just provides a convenient way to smooth and store the simulated distributions of $C - C_0$.

4 Response MAtrix: FI CCDs

4.1 Tweaks

Procedure is similar to that for the BI CCDs:

1. Simulate "ideal" rmfs
2. Simulate rmf with CTI and derive the scatter matrix
3. Extract 256x32 spectra
4. Fit them with RMF where the average shift of the scatter matrix is zero'ed.
5. Fit deviations to the CTI model (only parallel CTI unlike the case of BIs) and make improvements in the gain coefficients
6. Test on ECS
7. Test on E0102. Make the global low-E tweak if needed.

   I found that after the first cut, the following gain corrections (on average) are required:

E	Source	Correction
0.64	E0102, O-lines	+0.00%
0.95	E0102, Ne-lines	-0.80%
1.487	ECS, Al-Ka	-0.06%

   Approximate relation for correction:

   $$G = 1 - \frac{0.008}{1 + |E - 0.95|^3/0.253^3} \tag{4}$$

   (this makes a +0.1% correction at Al Ka).

   ```
   This is made by
      sh /data/alexey/cal/rmf/FI/mk_global_tweak_I > ! global_tweak_I.dat
   ```

8. Test again using the ECS and E0102 data:

E	Source	Correction	Scatter
0.64	E0102, O-lines	+0.3%	±0.7%
0.95	E0102, Ne-lines	+0.0%	±0.4%
1.487	ECS, Al-Ka	+0.04%	±0.2%
4.510	ECS, Ti-Ka	+0.08%	±0.17%
5.898	ECS, Mn-Ka	−0.07%	±0.10%

   GOOD ENOUGH!

9. recompute gains

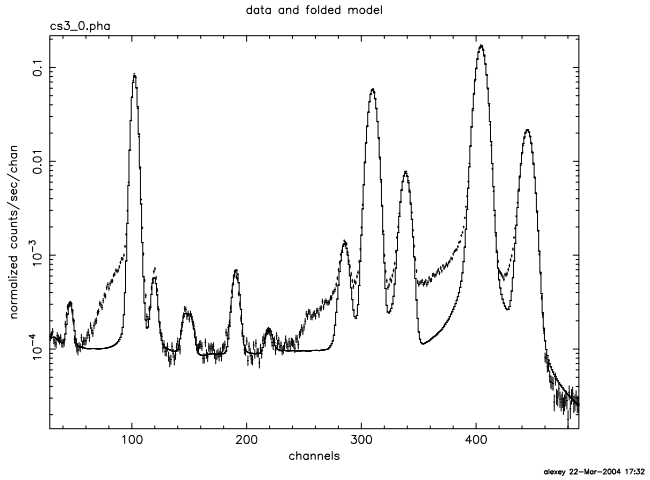

Fig. 2— Example of the ECS spectrum near the readout (CHIPY < 64 in I3). All lines have low-energy shoulders which are absent in the RMF model.

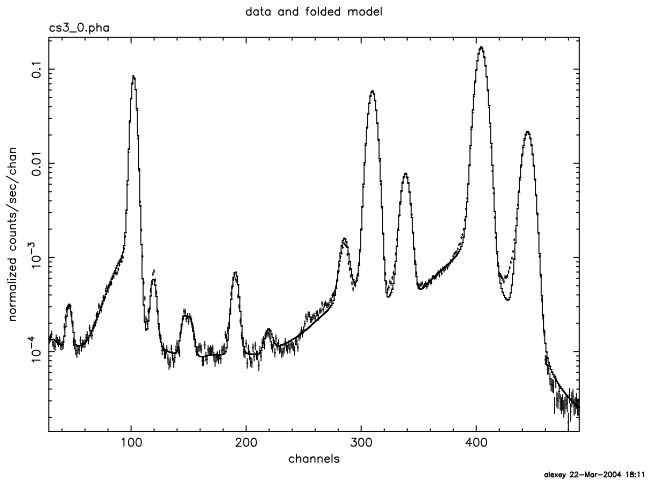

Fig. 3— The same as Fig. 2 but with exponential tails (eq.**???**) added to the RMF model.

10. Test for uniformity on Mn/Fe-L.

    EpochI: gain uniform within ±0.5% *rms* (consistent with statistical scatter); maximum deviations: −1.4%, +1.0%.

    EpochX: uniformity ±0.8% *rms* (consistent with statistical scatter); same average as in EpochI

5 Updates to the FI RMFs

5.1 Ideal response

Problem: ECS lines have low-energy spectral shoulders not adequately described by the MIT ACIS model (Fig. 2).

These shoulders are adequately fit with the modified exponential tail law,

$$f(E) = A \times \exp\left(-\frac{(E_0 - E)^\alpha}{\tau^\alpha}\right) \quad \text{for } E < E_0, \qquad f(E) = 0 \quad \text{for } E > E_0, \tag{5}$$

where E_0 equals to the line energy.

In all CCDs, the exponential tails adequately describe the data when the parameters are tied as follows

$$\begin{aligned} \alpha &= 2 \\ \tau &= 0.2334 \times E_{\rm keV}^{0.7} \\ \text{flux} &= (\text{Line Flux}) \times E_{\rm keV}^{-0.5} \times 0.056 \end{aligned} \tag{6}$$

At high energies, the absolute width of the tail increases, $w \propto \tau$ but the relative flux becomes small, $< 2.5\%$ for $E > 5keV$. At low energies, the relative flux increases, $f \sim 7\%$ for $E = 0.6 - 0.7$ keV, but the width of the tail because smaller.

Do we expect that the tail disapperars below some energy?

5.2 Scatter matrix

Problem: `add_cti.pro` does not adequately describe the wings in the CTI-induced response scatter.

Proposed modification: The scatter matrix is described by the following function:

$$R(E) = \begin{cases} (1 + (E - E_0)^2/\Delta^2)^{-\alpha_1} & \text{for } E < E_0 \\ (1 + (E - E_0)^2/\Delta^2)^{-\alpha_2} & \text{for } E > E_0 \end{cases} \tag{7}$$

The quantity 2Δ is somewhat equivalent to the FWHM of the line. The FI data are adequately described by

$$\alpha_1 = 3.70, \quad \alpha_2 = 1.90, \quad \text{and} \quad \delta \propto (E_0^{0.12} + 0.3 * E_0) \tag{8}$$

where E_0 is in keV.

The average energy for this equation ($\langle E \rangle = \int ER(E)\,dE / \int R(E)\,dE$) is

$$\langle E \rangle = E_0 + 0.2779\Delta \tag{9}$$

5.2.1 Derivation of the scatter matrix

Fit model to the data, smooth width(Y) with a polynomial fit, use eq. 8 to compute width for different energies at each location

5.2.2 Scatter matrix tweak

1. Extract 256x32 spectra
2. Fit them with RMF where the average shift of the scatter matrix is zero'ed (using eq. 9).
3. Fit deviations to the CTI + gain model and update the locations in the CTI scatter matrix.
4. Test on ECS
5. Test on E0102. Make the global low-E tweak if needed.

   I keep the tweak from original FI RMFs (see §4.1):

$$G = 1 - \frac{0.008}{1 + |E - 0.95|^3 / 0.253^3} \tag{10}$$

6. Test again using the ECS and E0102 data:

E	Source	Correction	Scatter
0.64	E0102, O-lines	+0.3%	±0.7%
0.95	E0102, Ne-lines	+0.0%	±0.4%
1.487	ECS, Al-Ka	−0.07%	±0.2%
4.510	ECS, Ti-Ka	+0.08%	±0.08%
5.898	ECS, Mn-Ka	−0.03%	±0.03%

   GOOD ENOUGH!

7. recompute gains
8. Test for uniformity on Mn/Fe-L.

   EpochI: gain uniform within ±0.5% *rms* (consistent with statistical scatter); maximum deviations: −1.4%, +1.0%.

   EpochX: uniformity ±0.8% *rms* (consistent with statistical scatter); same average as in EpochI

6 Response Matrix: BI CCDs

6.1 Making sense of the ACIS simulator

Simulate events in the node.

Shift in the Y direction at $X = 0$ gives parallel CTI. Shift in the X direction at $Y = 0$ gives serial CTI.

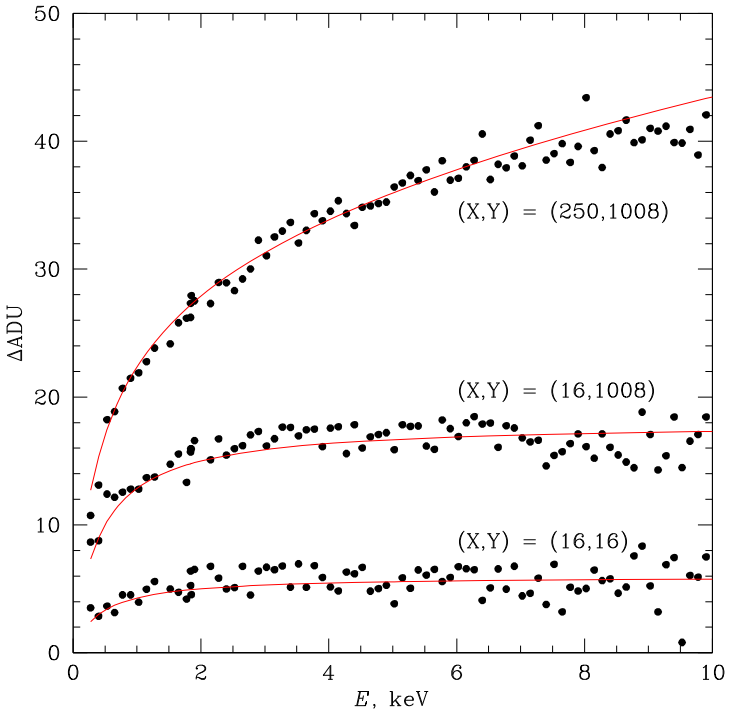

Fig. 4— Model for the parallel CTI

6.1.1 Parallel CTI

Parallel CTI is due to the charge loss in the Y direction.

Fig. 4 shows the change loss as a function of energy at the bottom of the node (x,y)=(16,16) and at the top of the node (x,y)=(16,1008). Charge loss is almost independent of energy. The following function gives a good fit:

$$\Delta\mathrm{ADU} = P \times \left(1 - \frac{0.4}{E_{\mathrm{keV}} + 0.4}\right), \tag{11}$$

where normalization constant is simply proportional to CHIPY.

6.1.2 Serial CTI

Serial CTI is due to the charge loss in the X direction.

Fig. 5 shows the change loss as a function of energy near the point (x,y)=(16,16) and near the opposite node boundary, (x,y)=(250,16). At the first point, the charge loss energy dependence is entirely due to the serial CTI. At high CHIPX, the charge loss is a strong function of energy which is an essential characteristic of the serial CTI. The following power law function gives a good description of the serial CTI as a funktion of energy:

$$\Delta\mathrm{ADU} = S \times E^{0.44} \tag{12}$$

where the normalization is simply proportional to CHIPX.

Finaly, we find that the total charge loss is simply the sum of the SERIAL and PARALLEL CTI effects (see the upper curve in Fig. 5).

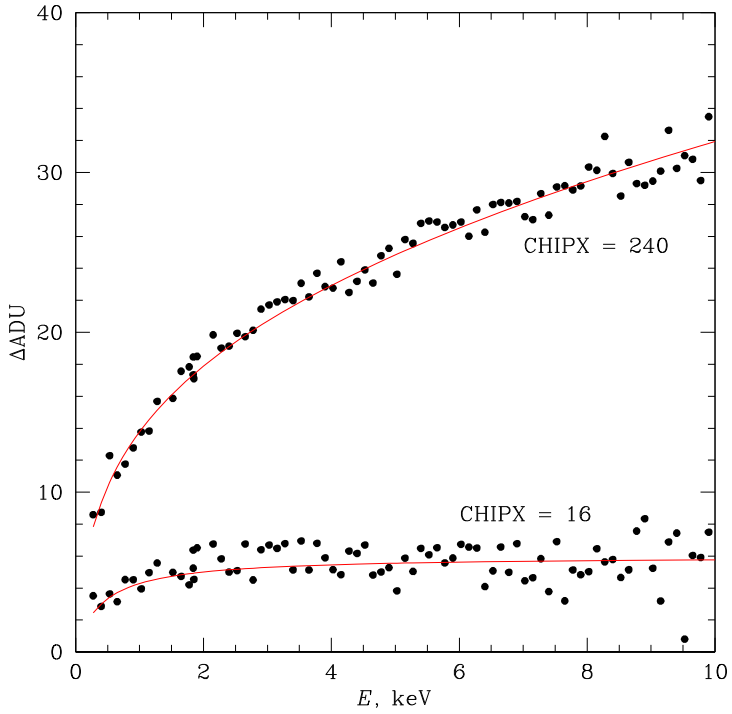

Fig. 5— Model for the serial CTI

6.1.3 *Degradation of the energy resolution*

$$\sigma_{\rm RMF} = \left(\sigma^2_{\rm ideal} + \sigma^2_{\rm CTI}\right)^{1/2} \tag{13}$$

Simulator suggests that $\sigma_{\rm CTI} \propto E^a$. ECS shows that $a \simeq 0.4$.

6.2 Calibration Procedure

1. Simulate "ideal" rmfs
2. Simulate rmf with CTI and derive models for the parallel and serial CTI
3. Extract 32x32 spectra
4. Fit them with ideal RMF (one RMF per node)
5. Fit deviations to the CTI model and make the scatter matrix without linear terms in the shifts.
   (a) record linear gain terms, modify the header of the pre-cti resp file, (it records the internal electronic gain and zero point shift on the per-node basis). Repeat step 4 and go to step 6
6. Fit deviations to the CTI model and make the scatter matrix including linear terms in the shifts.
7. Compute gains tables.
8. Test on ECS
9. Test on E0102. Make the global low-E tweak if needed.

   I found that after the first cut, the following gain corrections (on average) are required:

E	Source	Correction
0.64	E0102, O-lines	+2.3%
0.95	E0102, Ne-lines	+0.4%
1.487	ECS, Al-Ka	0.0 ± 0.2% (+0.45% max deviation)

   On average, this gain tweak is well-described by an exponential

$$G = 1 + 0.099 \exp(-(E/0.53)^2) \tag{14}$$

   At the Si edge, the tweak is close to zero.

```
This is made by
   sh /data/alexey/cal/rmf/BI.8-25-2003/mk_global_tweak > ! global_tweak_s3.dat
```

   Since the global tweak does not change the response at Al-Ka, we do not need to rerun step 8 with the RMFs, computed including the global tweak.
10. Test again using the ECS and E0102 data:

E	Source	Correction	Scatter
0.64	E0102, O-lines	+0.4%	±0.6%
0.95	E0102, Ne-lines	−0.0%	±0.4%
1.487	ECS, Al-Ka	+0.00%	±0.17%
4.510	ECS, Ti-Ka	+0.00%	±0.07%
5.898	ECS, Mn-Ka	+0.00%	±0.03%

    GOOD ENOUGH!
11. recompute gains
12. Test for uniformity on Mn/Fe-L.

    EpochI: gain uniform within ±0.6% *rms* (0.46% statistical); maximum deviations: −1.4%, +1.0%.

    Mean energy: 0.657 keV

6.3 S1

Global tweak: after the first-order tweak, average gain correction for Al is 0.3%. L-shell has an average energy of 0.6793; this a gain correction of 3.39%. Tweak:

$$G = 1 + 0.223 \times \exp(-E/0.35) \tag{15}$$

(0.1% at the Si edge).

The global tweak changes response at Al Ka, so I need to rerun the first-order tweak.

Apply TWEAK2 procedure

Test again using the ECS and E0102 data:

E	Source	Correction	Scatter
0.67	ECS, L-shell	+0.3%	±1.1% (max dev: ±3%
1.487	ECS, Al-Ka	+0.0%	±0.2%
4.510	ECS, Ti-Ka	+0.0%	±0.1%
5.898	ECS, Mn-Ka	+0.0%	±0.05%

GOOD ENOUGH!

7 BI CCDs with CTI correction

7.1 Energy resolution

Energy resolution is not completely flat as a function of Y. As a function of energy, it seems to follow a relation for non-cti-corrected data, $\sigma_{\rm cti} \propto E^{0.4}$.

7.2 Test results

E	Source	Correction	Scatter	Min/Max
1.487	ECS, Al-Ka	−0.02%	±0.15%	−0.61%, +0.47%
4.510	ECS, Ti-Ka	+0.00%	±0.07%	−0.13%, +0.11%
5.898	ECS, Mn-Ka	+0.01%	±0.05%	−0.10%, +0.14%

GOOD ENOUGH!

8 Gain tables

8.1 Definition and purpose

The term *gain table* is used in the *Chandra* data analysis to refer to the calibration product which establishes a relation between the measured pulse height amplitude (PHA) of the photons and their energies. This is achieved by assigning nominal PHA values, PHA_i to a set of input energies, E_i, and linear piece-wise interpolation of this table.

The energies are then used to assign the so called pulse-height independent channel (PI) to the photons. The definition in use is

$$\mathrm{PI} = [E/14.6\,\mathrm{eV}] + 1. \tag{16}$$

This procedure serves the following purposes listed in the decreasing order of importance

1. *(Critical)* The maximum of the spectral response to the photons of the same input energy can be located at very different PHA's depending on the CCD node and location within the node. The locations of the maxima expressed in PI channels should all be aligned by design. Therefore, the PI spectra from different regions can be combined without the loss of the spectral resolution.
2. *(Useful)* Assigned energies are useful for simple analysis tasks not requiring detailed spectral modelling, such as "to extract images in the 0.5–2 keV energy band".
3. *(Cosmetic)* The channel-to-energy conversion is used for plotting the spectral fits in popular packages such as XSPEC.

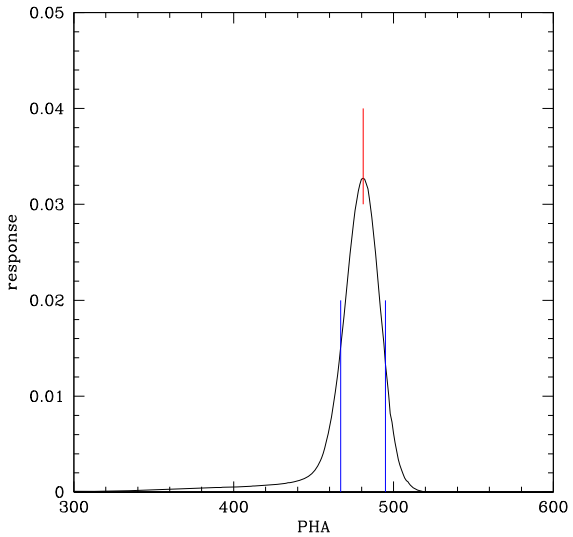

Fig. 6— Illustration of the peak measurement procedure for the gain calibration. Red line shows the measured PHA location, and the blue line show the FWHM window used in the iterative procedure (eq. 18).

8.2 Requirements

The purposes of the gain calibration outlined above imply the following requirements.

1. The correspondence between PHA channel and energy should be established using the most significant feature of the response — the main peak — because our main purpose is to align the spectra from different regions.
2. The relation between PHA and energy should be monotonic.
3. The assigned energies should be close to the true input energies. However, we note that some deviations from this rule are a) unavoidable (e.g., because the location of the main peak in the response is not a monotonic function of energy near 1.84 keV in the BI CCDs), and b) not harmful because the energies are not used for any quantative analysis; the only requirement here is that the deviations of the assigned from the input energy should be similar at all locations.
4. Gain relation should be smooth because otherwise it leads to spurious step-like features in the PI spectra —

$$\frac{d\,N}{d\,\mathrm{PI}} = \frac{d\,N}{d\,\mathrm{PHA}}\,\frac{d\,\mathrm{PHA}}{d\,\mathrm{PI}} \propto \frac{d\,N}{d\,\mathrm{PHA}}\,\frac{d\,\mathrm{PHA}}{d\,\mathrm{E}}. \tag{17}$$

   This requirement implies that the gain data should be approximated by a smooth function which should be tabulated with a sufficient resolution.

8.3 Measurements of PHA vs. Energy

The gain relation is derived from the RMFs in the following manner. Each row in the RMF image specifies the spectral response (flux per PHA channel) for the given input energy. First, the main peak is identified as the maximum of the response. Second, we determine FWHM of the peak (the window where the response is > 0.5 of the peak value). Finally, we find iteratively the average PHA channel within the FWHM window:

$$C = \mathrm{nint}\,(P^{(k)}); \quad P^{(k+1)} = \sum_{i=C-W/2}^{C+W/2} i\,R_i \;\times\; \left(\sum_{i=C-W/2}^{C+W/2} R_i\right)^{-1}, \tag{18}$$

where $P^{(k)}$ is the average value on the k-th iteration, W is the FWHM, and R_i is the response in the i-th PHA channel.

Effectively, this procedure find the peak location (but with greater than 1-channel accuracy) as illustrated in Fig. 6.

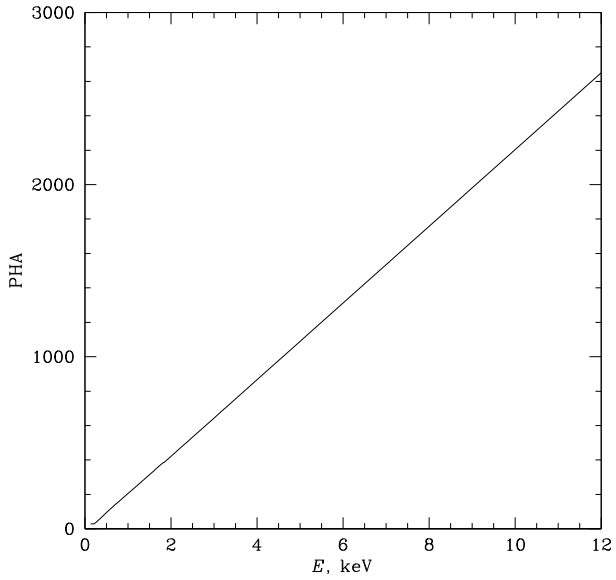

Fig. 7— PHA vs. energy in a typical location in the S3 chip.

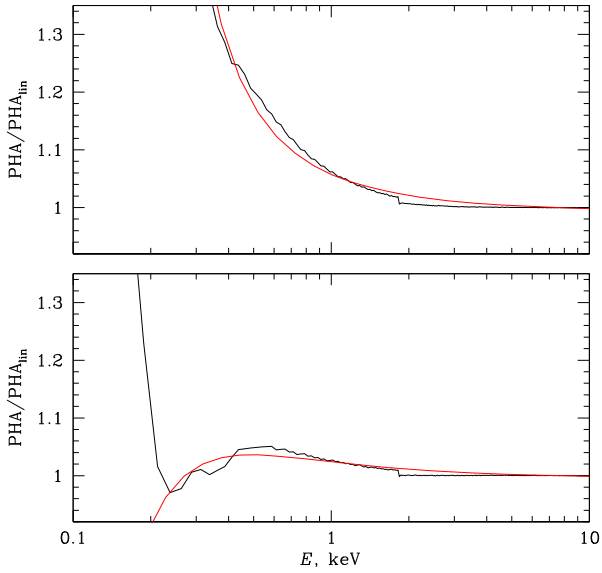

Fig. 8— Ratio of PHA vs. energy and the linear approximation of this relation near (CHIPX, CHIPY) = (16, 16) and (240, 1008) in the S3 chip (bottom and top panels, respectively).

8.4 Smooth approximation of the gain data

A typical relation of the PHA vs. input energy is shown in Fig. 7. The relation is very close to linear but a closer inspection reveals significant deviations from the linear fit. In Fig. 8, we show the ratios of the measured PHA vs. energy relation and its linear approximation in the 5–10 keV range. There are systematic deviations below 1 keV and also a step-like discontinuity near 1.84 keV, corresponding to the Si-K edge. The goal of the analytic fit described here is to smooth features such those near Si-K and adequately describe the low energy deviations.

We use the following function

$$\mathrm{PHA} = g \times E + s + \frac{a}{(E+c)^2}. \tag{19}$$

The function of this type always provide good fits to the measured relation (red lines in Fig. 8) at $E > (0.2 - 0.3)$ keV. At lower energies the response starts to "hit" the event threshold and the deviations become too large but $E < 0.3$ should not be used for spectral fits anyway.

There are systmatic deviations of the gain measurements from approximation (19), notably near 1.84 keV. As was noted before, such deviations are unavoidable. What is important is that *the fractional deviations are almost the same* at all locations as illustrated in Fig. 8. For the two locations shown in this Figure, the fractional deviations just above 1.84 keV is 1.5% and 1.3% or 28 and 24 eV, respectively. Therefore, we still achive the main purpose of the gain calibration which is to align the spectra from different CCD regions.

The calibration data files contain the best-fit functions (19) tabulated on a logarithmically spaced grid of energies in the 0.1–12 keV range (30 points in total).

References

[1] Bautz, M. W. & Nousek, J. A. (eds.), *Science Instrument Calibration Report for ACIS*, 1999, `http://cxc.harvard.edu/cal/Acis/cal_report.ps`.

[2] Townsley, L. K., Broos, P. S., Garmire, G. P., Nousek, J. A., *Mitigating Charge Transfer Inefficiency in the Chandra X-Ray Observatory Advanced CCD Imaging Spectrometer*, ApJ, 2000, 534, L139.

[3] Bautz, M., Ford, P., Grant, C., Kissel, S., LaMarr, B., Prigozhin, G., *ACIS CTI Correction Report*, 2001, `http://space.mit.edu/ACIS/cticor.ps`.

[4] Grant, C., Townsley, L., *CTI Correction Approaches*, 2001, http://space.mit.edu/ACIS/ctireport.ps.